Magnetic Circular Dichroism and Electron Paramagnetic Resonance Studies of Cobalt-Substituted Horse Liver Alcohol Dehydrogenase

Mark T. Werth,[†] Syou-Fen Tang,[†] Grazyna Formicka,[‡] Michael Zeppezauer,[‡] and Michael K. Johnson*,[†]

Department of Chemistry and Center for Metalloenzyme Studies, University of Georgia, Athens, Georgia 30602, and Fachrichtung 12.4 Biochemie, Universität des Saarlandes, P.O. Box 1150, D-66041 Saarbrücken, Germany

Received June 28, 1994[⊗]

The ground and excited state properties of Co(II) substituted for Zn(II) at the catalytic (c) and the noncatalytic (n) sites of horse liver alcohol dehydrogenase EE isozyme have been investigated by parallel EPR and UV/visible variable-temperature magnetic circular dichroism (VTMCD) spectroscopies. Samples were investigated as prepared and after formation of a ternary complex with NAD^+ and the potent inhibitor pyrazole. In accord with the structural role proposed for the noncatalytic metal, the spectroscopic properties of Co(II) at the noncatalytic site were unperturbed by formation of the ternary complex. The EPR spectra were readily analyzed in terms of a $S = {}^3/_2$ spin Hamiltonian using anisotropic intrinsic g-values in the range characteristic of tetrahedral Co(II), i.e. $g = 2.1-2.4$; $E/D \approx 0.33$, 0.05 (with $D < 0$), and 0 (with $D > 0$) for Co(c)Zn(n)-HLADH, Co(c)Zn(n)-HLADH/NAD^+/pyrazole, and Zn(c)Co(n)-HLADH, respectively. VTMCD studies facilitated resolution and assignment of S → Co(II) charge transfer bands (300-400 nm) and the components of the ${}^4A_2 \rightarrow {}^4T_1(P)$ tetrahedral d-d band (500-800 nm) that are split by spin-orbit coupling and low-symmetry distortions. The splittings of the highest energy d-d band are indicative of a much more distorted coordination environment for Co(II) at the catalytic site than the noncatalytic site. This is also reflected in the magnitude of ground state zero-field splitting, Δ, determined by analysis of the temperature dependence of discrete MCD bands, $|\Delta| = 33$, 56, and 7 cm^{-1} for Co(c)Zn(n)-HLADH, Co(c)Zn(n)-HLADH/NAD^+/pyrazole, and Zn(c)Co(n)-HLADH, respectively. MCD magnetization data are rationalized in terms of the EPR-determined ground state effective g-values, ground state zero-field splitting, and the polarization of the electronic transitions. The zero-field splittings for the samples with Co(II) at the catalytic site determined by VTMCD are quite different from those determined by EPR from the temperature dependence of the spin relaxation (Makinen, M. W.; Yim, M. B. *Proc. Natl. Acad. Sci. U.S.A.* **1981** *78*, 6221-6225), and the origin of this discrepancy is discussed. In accord with X-ray crystallographic studies, the EPR and VTMCD data are rationalized in terms of a highly distorted tetrahedral coordination environment for Co(II) at the catalytic site (two cysteines, one histidine, and one H_2O for Co(c)Zn(n)-HLADH and two cysteines, one histidine and one pyrazole for Co(c)Zn(n)-HLADH/NAD^+/pyrazole) and a more regular tetrahedral environment for Co(II) at the noncatalytic site (four cysteines).

Introduction

Horse liver alcohol dehydrogenase (HLADH)[1] is a dimeric enzyme ($M_r = 80\,000$) comprising two identical subunits each containing two zinc ions. The enzyme catalyzes the oxidation of primary and secondary alcohols to the corresponding aldehydes and ketones, respectively, using the coenzyme NAD^+. X-ray structures have been determined for the native enzyme as well as enzyme-coenzyme and enzyme-coenzyme-ligand/substrate ternary complexes.[2-9] Each subunit consists of two domains, referred to as the catalytic and the coenzyme domains, that form a deep cleft and are joined at a hinge region. NAD^+ or NADH binding occurs in the coenzyme domain and is necessary but not sufficient to induce a conformational change from an open to a closed form.[9] This conformational change entails rotation of the catalytic domain toward the coenzyme-binding domain resulting in a narrowing of the substrate channel and shielding of the coenzyme-binding region from the solvent medium.

One zinc ion is found buried deep in the catalytic domain near the hinge region and numerous studies have established that this "catalytic" zinc ion is the site of substrate binding.[7,10] In the absence of substrate or inhibitors, the catalytic zinc ion is coordinated by two sulfurs (Cys-46, Cys-176), one nitrogen (His-67), and one oxygen (water) in a distorted tetrahedral arrangement. A second zinc ion is found in the catalytic domain

* Corresponding author. Telephone: 706-542-9378. FAX: 706-542-9454. E-mail: johnson@sunchem.chem.uga.edu.
[†] University of Georgia.
[‡] Universität des Saarlandes.
[⊗] Abstract published in *Advance ACS Abstracts*, December 1, 1994.

(1) Abbreviations used: HLADH, horse liver alcohol dehydrogenase; VTMCD, variable-temperature magnetic circular dichroism; CT, charge transfer; Rd, rubredoxin; MT, metallothionein.

(2) Brändén, C.-I.; Jörnvall, H.; Eklund, H.; Furugen, B. *The Enzymes* **1975**, *11*, 103-190.
(3) Samama, J.-P.; Zeppezauer, E.; Biellmann, J.-F.; Brändén, C.-I. *Eur. J. Biochem.* **1977**, *81*, 403-409.
(4) Cedergren-Zeppezauer, E.; Samama, J.-P.; Eklund, H. *Biochemistry* **1982**, *21*, 4895-4908.
(5) Eklund, H.; Samama, J.-P.; Wallén, L.; Brändén, C.-I.; Akesson, A.; Jones, T. A. *J. Mol. Biol.* **1981**, *146*, 561-587.
(6) Cedergren-Zeppezauer, E. *Biochemistry* **1983**, *22*, 5761-5772.
(7) Eklund, H.; Brändén, C.-I. In *Zinc Enzymes*; Spiro, T. G., Ed.; Wiley: New York, 1983; pp 123-152.
(8) Eklund, H.; Jones, T. A.; Schneider, G. In *Zinc Enzymes*; Bertini, I., Luchinat, C., Maret, W., Zeppezauer, M., Eds.; Birkhäuser: Boston, Basel, Stuttgart, 1986; pp 377-392.
(9) Cedergren-Zeppezauer, E. In *Zinc Enzymes*; Bertini, I., Luchinat, C., Maret, W., Zeppezauer, M., Eds.; Birkhäuser: Boston, Basel, Stuttgart, 1986; pp 393-415.
(10) Zeppezauer, M. In *The Coordination Chemistry of Metalloenzymes*; Bertini, I., Drago, R. S., Luchinat, C., Eds.; D. Reidel Publishing Co.: Dordrecht, 1983; pp 99-122.

0020-1669/95/1334-0218$09.00/0

approximately 20 Å from the catalytic zinc ion. The observation that selective replacement of this zinc ion by other divalent metals has no effect on the enzymatic activity has led researchers to propose a structural role.[11-14] The coordination sphere of the structural or "noncatalytic" zinc is comprised of thiolate sulfur atoms from cysteines 97, 100, 103, and 111 in an approximately tetrahedral arrangement.

For more than three decades, the catalytic mechanism of HLADH has been the focus of intensive study. Unfortunately, Zn(II) is a d^{10} diamagnetic ion with uninformative electronic and magnetic properties. However, Zn(II) in either the catalytic or noncatalytic sites can be selectively substituted by other divalent metal ions with spectral and magnetic properties that are responsive to changes in the metal coordination sphere. Cobalt(II), which is generally high spin ($S = {}^3/_2$) in tetracoordinate and pentacoordinate environments with well-characterized electronic properties,[15] has been particularly useful in this regard, and methods have been devised for selectively substituting either the catalytic or noncatalytic Zn(II) by Co(II) with at least partial retention of catalytic activity.[13,14] Moreover, X-ray crystallographic studies of HLADH with Co(II) substituted at the catalytic site show that the protein structure and the coordination environment of the active site metal are essentially unperturbed compared to the native Zn enzyme.[16]

One aspect of the catalytic mechanism that is still somewhat controversial concerns the coordination number of the catalytic Zn during turnover.[9,16-18] Most researchers favor a mechanism in which the substrate displaces the active-site water molecule leaving the catalytic Zn site tetracoordinate. Indeed, a substantial body of evidence, including all the available X-ray crystallographic studies for binary and ternary complexes of native and Co(II)-substituted HLADH and the optical absorption data for binary and ternary complexes of Co(II)-substituted HLADH, supports the view that the active-site metal ion remains tetracoordinate throughout the catalytic cycle.[7,10,17,19,20] However, a pentacoordinate intermediate in which the substrate binds without displacement of water is central to the mechanisms proposed by Dworschak and Plapp[21] and Makinen and coworkers.[22] Spectroscopic evidence for pentacoordinate intermediate species comes from EPR studies of binary and ternary complexes of Co(II)-substituted HLADH[22-24] and perturbed angular correlation studies of ternary complexes of Cd(II)-substituted HLADH.[25] The EPR evidence comes from the magnitude of the ground state splitting, Δ, of high-spin Co(II) as determined by the temperature dependence of the spin-lattice relaxation.[26] On the basis of measurements of structurally defined Co(II) complexes, Makinen and co-workers have developed empirical relationships between the magnitude of Δ and the coordination number[27] from which they infer pentacoordination at the catalytic Co(II) site in binary complexes with NAD^+ and NADH and ternary complexes with NAD^+/pyrazole, NAD^+/CF_3CH_2OH, and $NADH/CF_3CH_2OH$.[22,23,27] Moreover, the effect of $H_2{}^{17}O$ on the EPR spin relaxation studies suggests that water remains coordinated in these ternary complexes.[22,24] One possible explanation for the apparently contradictory results from X-ray crystallography and optical absorption spectroscopy, on the one hand, and EPR, on the other, lies in the temperature of the measurements.[28] The cryogenic temperatures necessary for the EPR measurements may be responsible for stabilizing and/or promoting the formation of pentacoordinate species.

In this work we present a new approach to the problem of elucidating the excited state and ground state properties of Co(II) in Co(II)-substituted HLADH, i.e. variable-temperature magnetic circular dichroism (VTMCD) spectroscopy. We report VTMCD and EPR studies of HLADH selectively substituted with Co(II) at either the catalytic or noncatalytic site both as prepared and in closed-conformation ternary complexes with NAD^+ and pyrazole. In addition to providing a means of resolving and assigning the Co(II) ligand field transitions and assessing changes in coordination environment as a function of temperature, VTMCD measurements also afford an independent estimate of the magnitude of the ground state zero-field splitting that does not depend on the nature of the spin relaxation mechanism. The results do not support a change in Co(II) coordination number on formation of the ternary complex and rule out the possibility of tetracoordinate to pentacoordinate conversion in frozen samples. Moreover, they raise questions concerning the reliability of zero-field splittings determined by the EPR relaxation method and the utility of this parameter as a means of assessing the coordination number of high-spin Co(II) in low-symmetry biological environments.

Materials and Methods

Co(II)-Substituted Horse Liver Alcohol Dehydrogenase. Crystalline HLADH EE isozyme was prepared as previously described,[29] and the coenzyme NAD^+ was obtained from Boehringer (Mannheim, Germany). Selective substitution of Co(II) for Zn(II) at either the catalytic or noncatalytic site was performed using previously published methods.[13,14] Samples of Co(c)Zn(n)-HLADH and Zn(c)Co(n)-HLADH, which refer to Co(II) substituted into the catalytic and noncatalytic sites, respectively, were prepared in 50 mM Tes/Na^+ buffer, pH 7.5. Protein concentrations for Co(c)Zn(n)-HLADH and Zn(c)-Co(n)-HLADH were determined using $A_{280} = 0.56\ mg^{-1}\ cm^2$.[14,30] The sample concentrations given in the text and used in determining ϵ and $\Delta\epsilon$ values are based on the protein concentration and are expressed per subunit using $M_r = 40\,000$. Atomic absorption studies indicated that the degree of metal substitution was >93% for all the samples used in this work. To prevent oxidative degradation, all Co(II)-

(11) Drum, D. E.; Vallee, B. L. *Biochem. Biophys. Res. Commun.* **1970**, *41*, 33-39.
(12) Sytkowski, A. J.; Vallee, B. L. *Biochemistry* **1978**, *17*, 2850-2857.
(13) Maret, W.; Andersson, I.; Dietrich, H.; Schneider-Bernlöhr, H.; Einarsson, R.; Zeppezauer, M. *Eur. J. Biochem.* **1979**, *98*, 501-512.
(14) Formicka-Kozlowska, G.; Zeppezauer, M. *Inorg. Chim. Acta* **1988**, *151*, 183-189.
(15) Banci, L.; Bencini, A.; Benelli, C.; Gatteschi, D.; Zanchini, C. *Struct. Bonding* **1982**, *52*, 37-86.
(16) Schneider, G.; Eklund, H.; Cedergren-Zeppezauer, E.; Zeppezauer, M. *Proc. Natl. Acad. Sci. U.S.A.* **1983**, *80*, 5289-5293.
(17) Bertini, I.; Gerber, M.; Lanini, G.; Luchinat, C.; Maret, W.; Rawer, S.; Zeppezauer, M. *J. Am. Chem. Soc.* **1984**, *106*, 1826-1830.
(18) Makinen, M. W.; Kuo, L. C.; Yim, M. B.; Maret, W.; Wells, G. B. *J. Mol. Catal.* **1984**, *23*, 179-186.
(19) Corwin, D. T., Jr.; Fikar, R.; Koch, S. A. *Inorg. Chem.* **1987**, *26*, 3080-3082.
(20) Sartorius, C.; Dunn, M. F.; Zeppezauer, M. *Eur. J. Biochem.* **1988**, *177*, 493-499.
(21) Dworschak, R. T.; Plapp, B. V. *Biochemistry* **1977**, *16*, 2716-2725.
(22) Makinen, M. W.; Maret, W.; Yim, M. B. *Proc. Natl. Acad. Sci. U.S.A.* **1983**, *80*, 2584-2588.
(23) Makinen, M. W.; Yim, M. B. *Proc. Natl. Acad. Sci. U.S.A.* **1981**, *78*, 6221-6225.
(24) Yim, M. B.; Wells, G. B.; Kuo, L. C.; Makinen, M. W. In *Frontiers of Bioinorganic Chemistry*; Xavier, A. V., Ed.; VCH Publishers: Weinheim, 1986; pp 36-44.
(25) Andersson, I.; Bauer, R.; Demeter, I. *Inorg. Chim. Acta* **1982**, *67*, 53-59.
(26) Yim, M. B.; Kuo, L. C.; Makinen, M. W. *J. Magn. Reson.* **1982**, *46*, 247-256.
(27) Makinen, M. W.; Kuo, L. C.; Yim, M. B.; Wells, G. B.; Fukuyama, J. M.; Kim, J. E. *J. Am. Chem. Soc.* **1985**, *107*, 5245-5255.
(28) Bertini, I.; Luchinat, C.; Viezzoli, M. S. In *Zinc Enzymes*; Bertini, I., Luchinat, C., Maret, W., Zeppezauer, M., Eds.; Birkhäuser: Boston, Basel, Stuttgart, 1986; pp 27-47.
(29) Adolph, H. W. Ph.D. Thesis, University of Saarland, 1989.
(30) Adolph, H. W.; Maurer, P.; Schneider-Bernlöhr, H.; Sartorius, C.; Zeppezauer, M. *Eur. J. Biochem.* **1991**, *201*, 615-625.

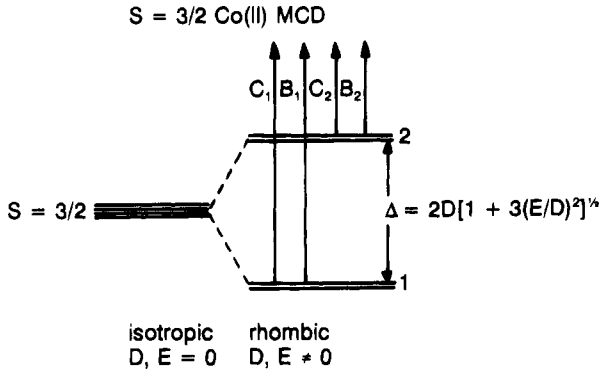

Figure 1. MCD bands originating from a $S = {}^3/_2$ ground state that is subject to rhombic zero-field splitting.

substituted HLADH samples were handled under an inert argon atmosphere in a Vacuum Atmospheres glovebox (<1 ppm of O_2). The ternary complex with NAD^+ and pyrazole was prepared by dialyzing enzyme (1.8−2.6 mM) against 50 mM Tris/HCl buffer, pH 7.5, containing 5 mM NAD^+ and 20 mM pyrazole. All samples for low-temperature MCD studies contained 50% (v/v) glycerol to ensure glass formation on freezing. The presence of 50% (v/v) glycerol induced no significant changes in the room-temperature absorption and CD spectra or the low-temperature EPR spectra of the Co(II)-HLADH samples investigated in this work.

Physical Measurements. The MCD spectrometer and experimental protocols for measuring spectra in the 180−1000 nm region at temperatures between 1.5 and 300 K and magnetic fields up to 5 T have been described elsewhere.[31,32] Sample temperatures were measured using calibrated carbon glass resistors (Lake Shore Cryogenics) positioned directly above and below the sample. The temperatures indicated by the resistance thermometers differed by <1% showing a negligible temperature gradient in the region of the sample, and the values quoted are the average of the two measurements. MCD spectra were recorded for samples in anaerobic 0.1 cm quartz cuvettes. The MCD spectra are shown after subtraction of the natural CD and are expressed as the difference in the molar extinction coefficients for left and right circularly polarized light, $\Delta\epsilon$, in units of M^{-1} cm^{-1}. The magnetic fields are given in the figure legends. Room-temperature optical absorption spectra of the MCD samples prior to freezing were recorded using a Hewlett-Packard 8452A diode array spectrophotometer.

Samples for EPR studies were frozen in liquid nitrogen at the same time as the MCD samples and stored in liquid nitrogen prior to measurement. X-band EPR spectra were recorded using a Bruker ER-220D EPR spectrometer interfaced to an IBM ESP 1600 computer. Low-temperature spectra were obtained by placing samples in an Oxford Instruments ESR-9 cryostat positioned in a TE_{102} cavity.

Results

EPR Spectra. The EPR spectra of high spin ($S = {}^3/_2$) Co(II) complexes are extremely sensitive to the coordination environment. However, while the observed g-values are readily interpreted in terms of a $S = {}^3/_2$ spin Hamiltonian,[33] they do not in themselves provide a means of discriminating among 4-, 5-, and 6-coordinations.[13] The $S = {}^3/_2$ ground state is split in zero field into two doublets by first- or second-order spin−orbit coupling and the magnitude of the zero-field splitting, Δ, is given by

$$\Delta = 2D\sqrt{(1 + 3(E/D)^2)} \qquad (1)$$

where D and E are the axial and rhombic zero-field-splitting parameters, respectively; see Figure 1. Since Δ is generally very much larger than the microwave energy, each doublet can be described in terms of a fictitious spin $S' = {}^1/_2$ using effective g'-values which are very sensitive to low-symmetry components of the ligand field. The g'-values correspond to the experimentally observed g-values and differ markedly from the true g-values, which are usually anisotropic and lie in the range 2.1−2.8 (2.1−2.4 for tetrahedral coordination). In the limit of axial symmetry, $g_\parallel' = g_\parallel$ and $g_\perp' = 2g_\perp$ for the $M_s = \pm{}^1/_2$ doublet and $g_\parallel' = 3g_\parallel$ and $g_\perp' = 0$ for the $M_s = \pm{}^3/_2$ doublet. A rhombic field mixes the two doublets such that the rigorous $M_s = \pm{}^3/_2$ or $\pm{}^1/_2$ designation is no longer appropriate, and the relationship between the effective and true g-values can be deduced from a first-order perturbation treatment[33]

$$g_x' = g_x\left[1 \pm \frac{1 + 3(E/D)}{\sqrt{(1 + 3(E/D)^2)}}\right]$$
$$g_y' = g_y\left[1 \pm \frac{1 - 3(E/D)}{\sqrt{(1 + 3(E/D)^2)}}\right]$$
$$g_z' = g_z\left[1 \mp \frac{2}{\sqrt{(1 + 3(E/D)^2)}}\right] \qquad (2)$$

where the upper and lower signs refer to the "$M_s = \pm{}^1/_2$" and "$M_s = \pm{}^3/_2$" doublets, respectively. These three equations, together with the relationship between E/D and the intrinsic g-values

$$\frac{E}{D} = \frac{g_x - g_y}{2g_z - (g_x + g_y)} \qquad (3)$$

enable estimates of the intrinsic g-values and E/D provided all three effective g-values are apparent in the EPR spectrum.

EPR spectra for the samples of Co(c)Zn(n)-HLADH and Zn(c)Co(n)-HLADH investigated in this work are shown in Figure 2. The resonances are extremely fast-relaxing such that they are only clearly visible below 15 K and were not significantly perturbed by the addition of 50% (v/v) glycerol, the medium used for the parallel VTMCD studies. The spectra of these Co(c)Zn(n)-HLADH and Zn(c)Co(n)-HLADH derivatives span the full range of EPR signals that can be observed for high-spin Co(II) centers.

In accord with previous studies,[23] Co(c)Zn(n)-HLADH exhibits a well-resolved rhombic spectrum, $g = 6.5$, 2.2, and 1.6, with ^{59}Co ($I = {}^7/_2$) hyperfine splitting apparent on only the low-field component. These effective g-values are indicative of high-spin Co(II) in a rhombically distorted environment. For example, for $g_x = 2.3$, $g_y = 2.2$, and $g_z = 2.1$, which translate into $E/D = 0.33$, the effective g-values are predicted to be 6.3, 2.2, and 1.6 for both doublets. Since the two Kramers doublets are completely mixed by the rhombic field (i.e. $E/D = 0.33$), the sign of D, which dictates which of the two doublets is lowest in energy for an axial field, is irrelevant.

A very different EPR spectrum is observed for the Co(c)-Zn(n)-HLADH/NAD^+/pyrazole ternary complex. The sole discernible feature for temperatures in the range 4.2−15 K and microwave powers between 1 and 100 mW, is a low-field absorption-shaped component centered at $g = 7.1$ with well-resolved ^{59}Co hyperfine splitting. The resonance increased in intensity with decreasing temperature down to 4.2 K, indicating that it arises from the lower doublet. These properties, particularly the large hyperfine splitting,[15] indicate that the

(31) Kowal, A. T.; Zambrano, I. C.; Moura, I.; Moura, J. J. G.; LeGall, J.; Johnson, M. K. *Inorg. Chem.* **1988**, *27*, 1162−1166.
(32) Johnson, M. K. In *Metal Clusters in Proteins*; Que, L., Jr., Ed.; ACS Symposium Series 372; American Chemical Society: Washington, DC, 1988; pp 326−342.
(33) Pilbrow, J. R. *J. Magn. Reson.* **1978**, *31*, 479−489.

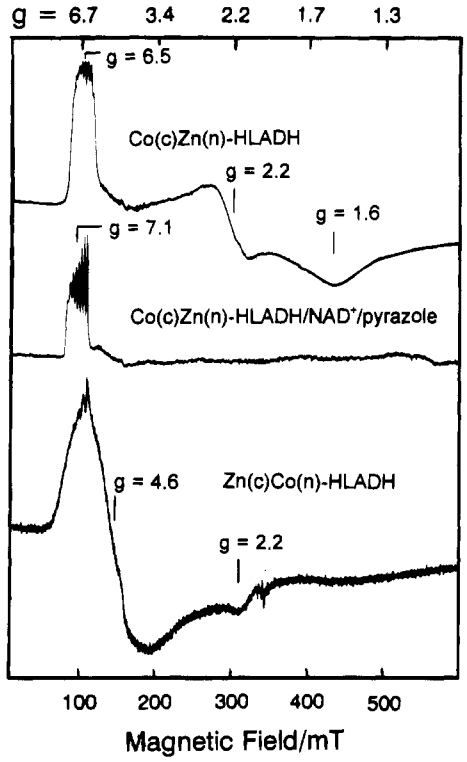

Figure 2. EPR spectra of Co(II)-substituted HLADH derivatives: Co(c)Zn(n)-HLADH, 1.6 mM in 50 mM Tes/Na^+ buffer, pH 7.5; Co(c)Zn(n)-HLADH/NAD^+/pyrazole ternary complex, 1.3 mM in 50 mM Tris/HCl buffer, pH 7.5, prepared as described under Materials and Methods; Zn(c)Co(n)-HLADH, 1.2 mM in 50 mM Tes/Na^+ buffer, pH 7.5. Conditions of measurement: temperature, 7 K; microwave power, 10 mW; modulation amplitude, 0.63 mT; microwave frequency, 9.41 GHz.

resonance occurs within the $M_s = \pm^3/_2$ doublet of an $S = {}^3/_2$ ground state that is subject to large and predominantly axial zero-field splitting with $D < 0$. The transition probability is much larger for resonance within the upper $M_s = \pm^1/_2$ doublet. Hence the zero-field splitting must be large in order to explain the absence of such resonances at higher temperatures prior to the onset of line width broadening resulting from rapid relaxation. In the limit of a rigorously axial environment ($E/D = 0$), the transition probability is zero for resonance within the $M_s = \pm^3/_2$ doublet ($g_{\|}' = 3g_{\|}$ and $g_{\perp}' = 0$). However, it will become finite if some rhombic anisotropy is introduced. While a unique solution to the spin Hamiltonian is not possible since the high-field components of the resonance are too broad to observe, it is worthwhile to consider a plausible set of ground parameters in order to understand the origin of the observed spectrum. For example, $g_x = 2.20$, $g_y = 2.18$, and $g_z = 2.40$, which dictate $E/D = 0.05$, and $D < 0$, result in effective g-values of 4.7, 4.0, 2.4 and 7.2, 0.3, 0.3 for the upper ("$M_s = \pm^1/_2$") and lower ("$M_s = \pm^3/_2$") doublets, respectively. The EPR spectrum observed for the Co(c)Zn(n)-HLADH/NAD^+/pyrazole complex in this work is *completely* different from that reported previously by Makinen and Yim ($g_{\perp} \approx 4.7$ and $g_{\|} \approx 2.7$).[23] The origin of this discrepancy is unclear. However, it should be noted that no UV/visible absorption data to support the formation of the Co(c)Zn(n)-HLADH/NAD^+/pyrazole ternary complex were presented by these authors. In contrast, the samples used in this work exhibited the characteristic absorption spectrum of this ternary complex[34] (see below) both before and after EPR measurements.

(34) Koerber, S. C.; MacGibbon, A. H. K.; Dietrich, H.; Zeppezauer, M.; Dunn, M. F. *Biochemistry* **1983**, *22*, 3424–3431.

The EPR spectra clearly reveal dramatic changes in the ground state properties of Co(II) in the catalytic site of HLADH upon the formation of the ternary complex with NAD^+ and pyrazole. In contrast, the EPR spectrum of Co(II) in the noncatalytic site was not significantly perturbed by ternary complex formation. The EPR spectrum of Zn(c)Co(n)-HLADH (see Figure 2) comprises a broad derivative centered at $g = 4.6$ and a negative feature centered at $g = 2.2$. The resonance increases in intensity with decreasing temperature over the range 4.2–15 K. It is therefore readily interpreted in terms of an axial $S = {}^3/_2$ ground state, $E/D = 0$ and $D > 0$, with intrinsic g-values $g_{\|} = 2.2$ and $g_{\perp} = 2.3$. A very similar resonance was observed for the Zn(c)Co(n)-HLADH/NAD^+/pyrazole ternary complex (data not shown).

UV/Visible Absorption and VTMCD Spectra. Room-temperature UV/visible absorption spectra and VTMCD spectra of Co(c)Zn(n)-HLADH, the Co(c)Zn(n)-HLADH/NAD^+/pyrazole ternary complex, and Zn(c)Co(n)-HLADH are shown in Figures 3–5, respectively. The absorption spectra are quantitatively in agreement with those published previously for these Co(II)-substituted HLADH derivatives.[13,14,34] The spectra comprise intense bands between 300 and 450 nm that are assigned to ligand-to-metal charge transfer transitions (predominantly S → Co(II) charge transfer) and weaker bands between 500 and 800 nm that are assigned to components of the highest energy ligand field transition, $^4A_2 \rightarrow {}^4T_1(P)$,[35] under idealized tetrahedral symmetry; see Table 1. Empirical observations for Co(II) complexes with well-defined coordination spheres suggest that the molar extinction coefficient (M^{-1} cm^{-1}) of the most intense ligand field band can be used as an indicator of coordination number: $\epsilon < 50$, six-coordinate; $50 < \epsilon < 300$, five-coordinate; $\epsilon > 300$, four-coordinate.[15,19,38] On the basis of this criterion, all three Co(II)-substituted HLADH samples investigated in this work are four-coordinate.

Temperature-dependent MCD bands, *C*-terms, underlie the absorption bands and facilitate resolution of discrete transitions. Indeed the close correspondence between the energies of the room-temperature absorption bands and the temperature-dependent MCD bands provides evidence against changes in the Co(II) coordination environment on freezing samples for EPR and VTMCD spectroscopies. This is confirmed by low-temperature absorption studies (1.6 K) of the samples used for VTMCD studies, which show sharpening but no significant shifts of the absorption bands (data not shown). It is also apparent from the temperature dependence of the spectra shown in Figures 3–5 and spectra recorded at higher temperatures, that *B*-terms dominate the room-temperature MCD spectra of the samples with Co(II) in the catalytic site whereas *C*-terms dominate the room-temperature MCD spectra of the samples with Co(II) in the noncatalytic site. In addition to highlighting the limitations of room-temperature MCD for investigating electronic transitions, this observation has important consequences for interpreting MCD magnetization and temperature dependence studies in terms of ground state parameters; see below.

Tentative assignments for the MCD bands in the charge transfer region, based on the expected order of the ligand valence electronic levels, i.e. $\pi N < \sigma S < \pi S$, are given in Table 1. For

(35) Garmer, D. R.; Krauss, M. *J. Am. Chem. Soc.* **1993**, *115*, 10247–10257 and references therein.

(36) Dixon, B. A. Ph.D. Thesis, Louisiana State University, 1987.

(37) Moura, I.; Teixeira, M.; LeGall, J.; Moura, J. J. G. *J. Inorg. Biochem.* **1991**, *44*, 127–139.

(38) Bertini, I. In *Coordination Chemistry of Metalloenzymes*; Bertini, I., Drago, R. S., Luchinat, C., Eds.; D. Reidel Publishing Co.: Dordrecht, 1983; pp 1–18.

Table 1. Room-Temperature Absorption and Variable-Temperature MCD Data (nm) for Co-Substituted Alcohol Dehydrogenase, Rubredoxin, and Metallothionein[a]

	Co(c)Zn(n)-HLADH		Co(c)Zn(n)-HLADH/NAD$^+$/pyrazole		Zn(n)Co(c)-HLADH		Co-MT[b]		Co-Rd[c]	
assign	abs	VTMCD	abs	VTMCD	abs	VTMCD	abs	VTMCD	abs	VTMCD
σS → Co(II) CT		320(−122)		339 (−55)		324 (−320)	305 (4.0)	320 (−250)		
πS → Co(II) CT	340 (3.5)	344 (−105)	388 (1.8)	385 (−50)	341 (3.0)	340 (−300)		338 (−220)	350 (3.3)	343 (−550)
πS → Co(II) CT	385 (sh)	376 (+152)	428 (sh)	422 (+190)	367 (sh)	360 (−130)	360 (sh)	372 (+160)	370 (sh)	366 (+400)
πS → Co(II) CT						383 (+230)				
Co(II) d−d $^4A_2 \rightarrow {}^4T_1(P)$	520 (0.2)	550 (−20)	528 (0.4)	527 (−60)	625 (sh)	625 (+30)	615 (0.2)	610 (+20)	623 (0.3)	626 (−60)
	655 (0.6)	633 (sh)	646 (0.5)	633 (−100)	663 (0.5)	666 (−180)	685 (0.4)	668 (−150)	665 (0.4)	650 (−140)
		662 (−220)	678 (0.6)	674 (−150)	740 (0.3)	733 (−180)	740 (0.3)	715 (−130)	690 (0.5)	676 (−180)
									745 (0.7)	723 (−200)

[a] ϵ values for the absorption bands in units of mM^{-1} cm^{-1} and $\Delta\epsilon$ values for the MCD bands at 4.5 T and 4.2 K in units of M^{-1} cm^{-1} are given in parentheses; sh indicates shoulder. [b] Rabbit liver apometallothionein with 1 equiv of Co(II). Data taken from ref 36. [c] Co(II)-substituted rubredoxin from *Desulfovibrio gigas*. Data taken from refs 36 and 37.

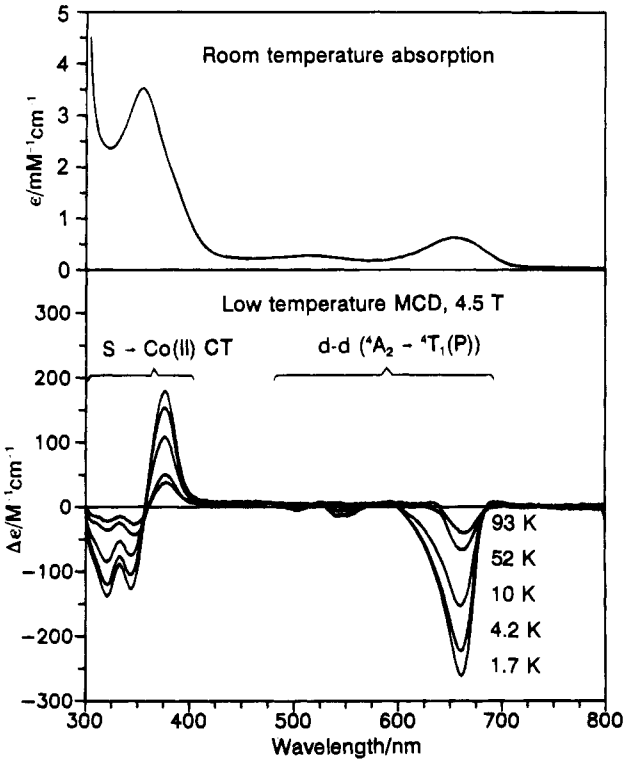

Figure 3. Room-temperature absorption and variable-temperature MCD spectra of Co(c)Zn(n)-HLADH, 0.35 mM in 50 mM Tes/Na$^+$ buffer, pH 7.5, with 50% (v/v) glycerol. Upper panel: room-temperature absorption. Lower panel: MCD spectra recorded with a magnetic field of 4.5 T at 1.66, 4.22, 10.6, 52, and 93 K. The intensity of all MCD bands increases with decreasing temperature.

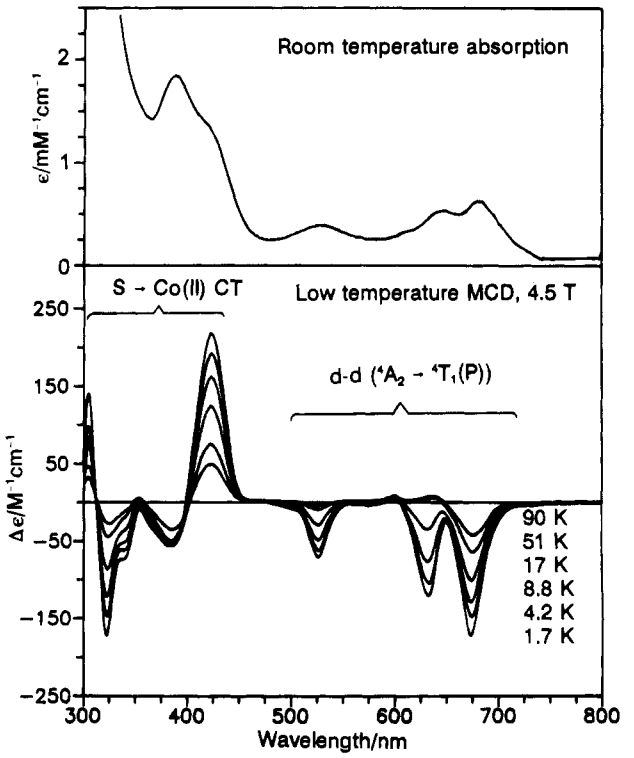

Figure 4. Room-temperature absorption and variable-temperature MCD spectra of the Co(c)Zn(n)-HLADH/NAD$^+$/pyrazole ternary complex, 0.62 mM in 50 mM Tris/HCl buffer, pH 7.5, prepared as described under Materials and Methods, with 50% (v/v) glycerol. Upper panel: room-temperature absorption. Lower panel: MCD spectra with a magnetic field of 4.5 T at 1.66, 4.22, 8.8, 17.4, 51, and 90 K. The intensity of all bands increases with decreasing temperature.

the samples with Co(II) substituted at the catalytic site, contributions from πN(His) → Co(II) charge transfer to the highest energy transitions cannot be ruled out. However, since similar MCD spectra are observed for tetrahedral Co(II) sites with complete cysteinyl-*S* coordination, i.e. Zn(c)Co(n)-HLADH, Co-substituted rubredoxin, and apometallothionein with a 1 equiv of Co(II), it seems more likely that πN(His) → Co(II) charge transfer transitions occur at wavelengths <300 nm. Pyrazole binding to Co(II) at the catalytic site results in new MCD bands at 304 nm ($\Delta\epsilon$ = +100 M^{-1} cm^{-1} at 4.2 K and 4.5 T) and 323 ($\Delta\epsilon$ = −150 M^{-1} cm^{-1} at 4.2 K and 4.5 T) that are attributed to πN(pyrazole) → Co(II) charge transfer and a shift in the πS(Cys) → Co(II) charge transfer bands to lower energy.

The energies and signs of the MCD bands corresponding to the highest energy ligand field transition, $^4A_2 \rightarrow {}^4T_1(P)$, are similar for the tetrahedral Co(II) centers with complete cysteinyl-*S* coordination in Zn(c)Co(n)-HLADH, Co-substituted rubredoxin, and apometallothionein with 1 equiv of Co(II). For Zn(c)Co(n)-HLADH, the absorption and MCD spectra show that the $^4T_1(P)$ excited state is split into at least three components with an average energy of 14 900 cm^{-1} (671 nm). The energy separation between the components and the signs of the MCD bands are consistent with first-order spin−orbit coupling as the dominant contributor to the excited state splitting (the spin−orbit coupling constant for Co(II) complexes is typically 500 cm^{-1}) rather than low-symmetry distortions.[39,40] This is consistent with a coordination geometry approaching idealized tetrahedral.

(39) Lomenzo, J. A.; Bird, B. D.; Osborne, G. A.; Stephens, P. J. *Chem. Phys. Lett.* **1971**, *9*, 332−336.
(40) Katô, H.; Akimoto, K. *J. Am. Chem. Soc.* **1974**, *96*, 1351−1357 and references therein.

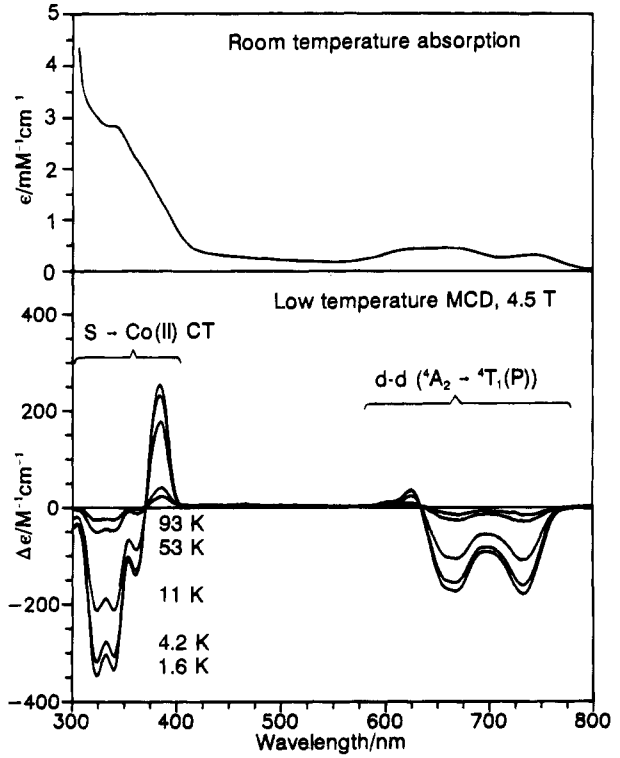

Figure 5. Room-temperature absorption and variable-temperature MCD spectra of Zn(c)Co(n)-HLADH, 0.31 mM in 50 mM Tes/Na^+ buffer, pH 7.5, with 50% (v/v) glycerol. Upper panel: room-temperature absorption. Lower panel: MCD spectra recorded with a magnetic field of 4.5 T at 1.63, 4.22, 10.6, 53, and 93 K. The intensity of all bands increases with decreasing temperature.

The highest energy set of ligand field transitions has larger splittings and occurs at significantly higher energies for the samples of HLADH with Co(II) at the catalytic site; see Table 1. Indeed, it is not possible to rule out five-coordinate Co(II) sites based solely on the energies and splittings of the observed d−d bands.[15] However, since the ordering of the potential ligands in the spectrochemical series is pyrazole ≈ histidine > H_2O > cysteine, the average energies of the MCD *C*-terms, 16 360 cm^{-1} (611 nm) for Co(c)Zn(n)-HLADH and 16 540 cm^{-1} (605 nm) for the Co(c)Zn(n)-HLADH/NAD^+/pyrazole ternary complex, are consistent with the anticipated increase in tetrahedral ligand field strength associated with changing to ligand donor sets comprising two cysteines, one histidine, and one H_2O or two cysteines, one histidine, and one pyrazole. Hence the intense temperature-dependent negative MCD band at 662 nm with a high-energy shoulder at ≈633 nm and the weaker negative MCD band centered at 550 nm in Co(c)Zn(n)-HLADH are assigned to components of the $^4A_2 \rightarrow {}^4T_1(P)$ d−d transition. The magnitude of the energy separation between the components dictates that low-symmetry distortions are primarily responsible for the excited state splitting. The very weak negative MCD band at 506 nm is tentatively assigned to a spin-forbidden, quartet-to-doublet d−d band. Such spin-forbidden d−d bands gain intensity by mixing with nearby $^4T_1(P)$ state and are frequently observed in the MCD spectra of tetrahedral Co(II) complexes.[39,40] In addition, they contribute to the broad and weak absorption feature centered at 520 nm. Single-crystal polarized absorption studies of Co(c)Zn(n)-HLADH indicate that the 520 and 655 nm absorption bands are predominantly *z*-polarized and *xy*-polarized, respectively.[41] Since MCD *C*-terms require two perpendicular, non-zero

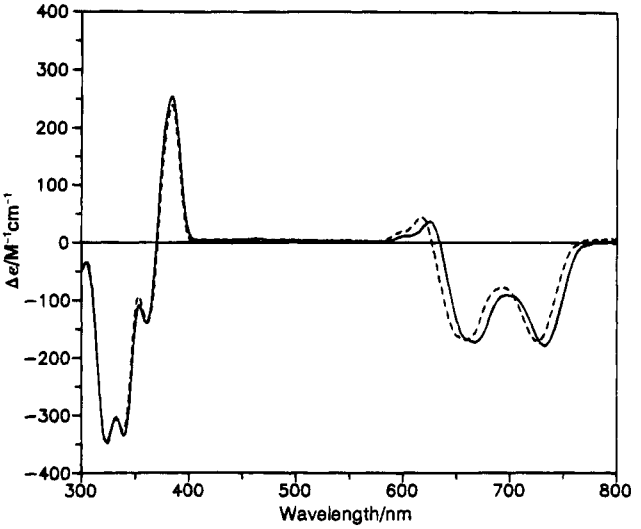

Figure 6. Comparison of the low-temperature MCD spectra of Zn(c)Co(n)-HLADH (solid line) and the Zn(c)Co(n)-HLADH/NAD^+/pyrazole ternary complex (broken line) . The Zn(c)Co(n)-HLADH sample is as described in the caption of Figure 5. The ternary complex sample, 0.42 mM in 50 mM Tris/HCl buffer, pH 7.5, was prepared as described under Materials and Methods and contained 50% (v/v) glycerol. MCD spectra were recorded with a magnetic field of 4.5 T at 1.6 K

transition moments for significant intensity, much larger temperature-dependent MCD intensity is expected and observed under the 655 nm band.

Pyrazole binding in place of water also results in a very distorted tetrahedral coordination environment as evidenced by the large splitting of the $^4A_2 \rightarrow {}^4T_1(P)$ d−d band into three well-resolved components that exhibit intense negative *C*-terms centered at 527, 633, and 674 nm. The average energy, 16 540 cm^{-1}, is close to those observed for the Co(II) complex of a zinc finger consensus peptide, 16 580 cm^{-1},[42] and $Co[SC(CH_3)_2CH_2NH_2]_2$, 16 475 cm^{-1},[41] both of which have tetrahedral coordination for the S_2N_2 donor set. Furthermore, the absorption spectrum of the Co(c)Zn(n)-HLADH/NAD^+/pyrazole ternary complex is almost identical to that of the model compound [Co(S-2,4,6-*i*-$Pr_3C_6H_2)_2$(1-Me-imid)$_2$], which has a highly distorted tetrahedral structure for the S_2N_2 donor set as a result of the extremely bulky thiolate groups.[19]

In accord with the EPR results, inhibitor binding at the catalytic site and ternary complex formation with concomitant closure of conformation have little effect on the metal coordination at the noncatalytic site as evidenced by the VTMCD spectra of Zn(c)Co(n)-HLADH and the Zn(c)Co(n)-HLADH/NAD^+/pyrazole ternary complex; see Figure 6. The charge transfer region is unchanged in the ternary complex, and the d−d bands all undergo a small shift to higher energy without any significant change in sign or relative intensity.

Ground State Properties from VTMCD Measurements. Detailed studies of the temperature and magnetic field dependence of discrete MCD bands provide a means of investigating the properties of the $^4A_2$ ground state that is complementary to EPR, and independent of spin relaxation effects. To assess the zero-field splitting, the temperature dependence of the MCD intensity was investigated at small applied fields.[43,44] In the linear limit, i.e. $kT \gg g\beta B$ and $\Delta\epsilon$ linearly dependent on B,

(41) Makinen, M. W.; Hill, S. C.; Zeppezauer, M.; Little, C. L.; Burdett, J. K. *J. Am. Chem. Soc.* **1987**, *109*, 4072−4081.
(42) Krizek, B. A.; Amann, B. T.; Kilfoil, V. J.; Merkle, D. L.; Berg, J. M. *J. Am. Chem. Soc.* **1991**, *113*, 4518−4523.
(43) Browett, W. R.; Fucaloro, A. F.; Morgan, T. V.; Stephens, P. J. *J. Am. Chem. Soc.* **1983**, *105*, 1868−1872.
(44) Johnson, M. K. In *Physical Methods in Inorganic and Bioinorganic Chemistry*; Que, L., Ed.; University Science: Mill Valley, CA; in press.

plots of $\Delta\epsilon$ versus $1/T$ will deviate from linear if low-lying states are populated with increasing temperature. In all three samples investigated in this work, the MCD intensity was found to be linear in B up to 1 T and applied fields between 0.5 and 1 T were used for these measurements. Plots of the MCD intensity in arbitrary units versus $1/T$ for Co(c)Zn(n)-HLADH at 662 nm, Co(c)Zn(n)-HLADH/NAD^+/pyrazole at 674 nm, and Zn(c)Co(n)-HLADH at 733 nm are shown in Figure 7. The MCD intensity is proportional to the sum of the C-term and B-term contributions from each doublet weighted according to the fractional population of each doublet (see Figure 1), i.e.

$$\Delta\epsilon \propto \alpha_1\left(B_1 + \frac{C_1}{kT}\right) + (1 - \alpha_1)\left(B_2 + \frac{C_2}{kT}\right) \qquad (4)$$

$$\alpha_1 = \frac{1}{1 + \exp\left(-\frac{\Delta}{kT}\right)}$$

The solid lines are the best fits to eq 4 using a nonlinear least-squares fitting procedure, and the best-fit parameters are given in Figure 7. Using this procedure, the zero-field splittings, Δ, were determined to be 33 ± 4, -56 ± 6, and $+7 \pm 4$ cm^{-1} for Co(c)Zn(n)-HLADH, Co(c)Zn(n)-HLADH/NAD^+/pyrazole, and Zn(c)Co(n)-HLADH, respectively. (This procedure determines only the absolute value of Δ. For predominantly axial ground states, the sign of D is important in determining ground state properties, and the signs indicated come from the analysis of the EPR data given above.) These values of Δ are quite different from those reported previously for Co(c)Zn(n)-HLADH and Co(c)Zn(n)-HLADH/NAD^+/pyrazole on the basis of analysis of the temperature dependence of the spin–lattice relaxation, i.e. +9 and +47 cm^{-1}, respectively.[23] In addition, they are well out of the range established by Makinen and co-workers for tetrahedral Co(II) centers, -36 to $+13$ cm^{-1}.[27] Consequently, in order to test the uniqueness of the Δ values determined in this work, similar experiments were conducted at 376 nm for Co(c)Zn(n)-HLADH, 422 and 633 nm for Co(c)Zn(n)-HLADH/NAD^+/pyrazole, and 383 and 666 nm for Zn(c)Co(n)-HLADH (data not shown). In each case, values within 10% of those given above were obtained.

At the wavelengths shown in Figure 7, significant B-term contributions were required to fit the data obtained for Co(c)-Zn(n)-HLADH and Co(c)Zn(n)-HLADH/NAD^+/pyrazole. However, in both cases, the magnitude of the B-term contribution is entirely consistent with that required for interpretation of the MCD magnetization data at these wavelengths; see below. Since the B-term contributions from the two doublets are almost equal in magnitude, but opposite in sign, field-induced mixing between the doublets of the ground state manifold is responsible for the B-term contribution. In essence, this is a temperature-dependent B-term contribution, since the mixing state itself becomes populated over the temperature range of the experiment.[44]

MCD magnetization or saturation curves, i.e. plots of MCD intensity to magnetic saturation at a variety of fixed temperatures as a function of magnetic field, can provide information about the ground state g-values and transition polarizations for isolated Kramers doublets.[44] Magnetization plots for all three of the Co(II)-HLADH derivatives investigated in this work at the same wavelengths used for the temperature dependence studies are shown in Figure 8. In all three plots, the raw data (left panels) are "nested" with field dependence studies at different fixed temperatures lying on separate curves. Such behavior is characteristic of $S > {}^1/_2$ ground states that are subject to zero-field splitting as a result of first- or second-order spin–orbit coupling and is a consequence of field-induced mixing within the ground state manifold (B-terms) and/or the Boltzmann population distribution over the ground state manifold. In light

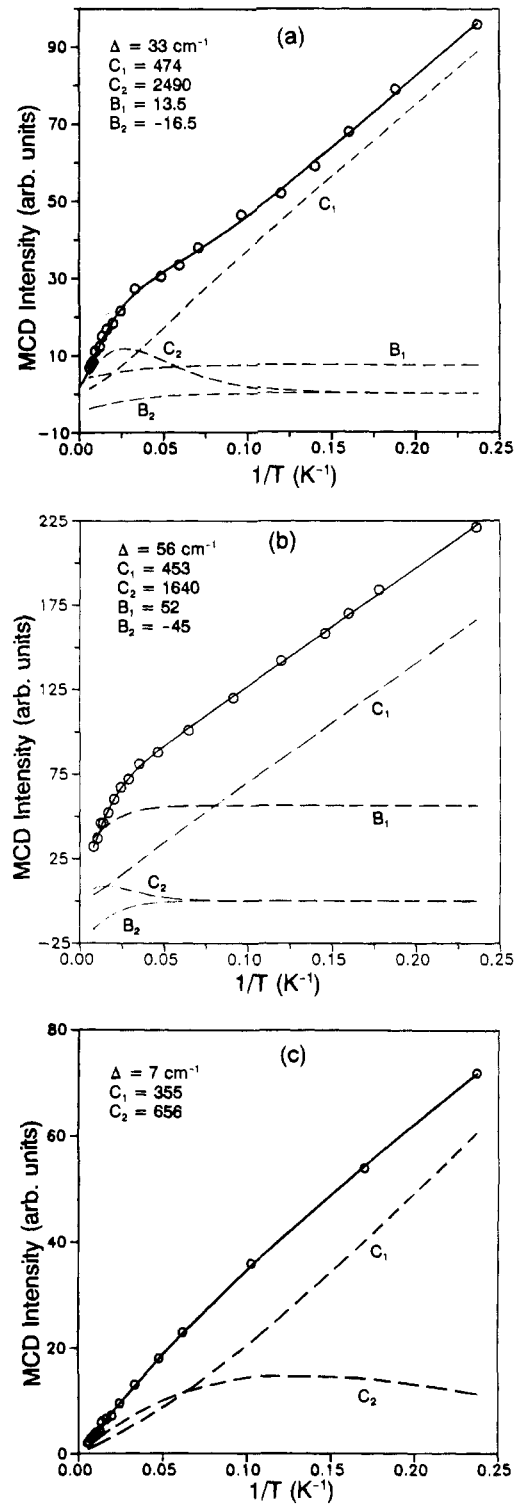

Figure 7. MCD temperature dependence of Co(II)-substituted HLADH derivatives: (a) Co(c)Zn(n)-HLADH at 662 nm with a magnetic field of 0.5 T; (b) Co(c)Zn(n)-HLADH/NAD^+/pyrazole ternary complex at 674 nm with a magnetic field of 1.0 T; (c) Zn(c)Co(n)-HLADH at 733 nm with a magnetic field of 0.5 T. Circles are experimental data. The solid lines are the best fit to eq 4, and the best fit parameters are indicated on each plot. Δ is the zero-field splitting between the ground state doublets. C_1, C_2, B_1, and B_2 have arbitrary units and indicate only the relative values of the C-terms and B-terms originating from the upper (2) and lower (1) doublets of the ground state manifold. Non-zero values of B_1 and B_2 did not improve the fit in (c). The broken lines show the C-term and B-term contributions from the two doublets of the $S = {}^3/_2$ ground state.

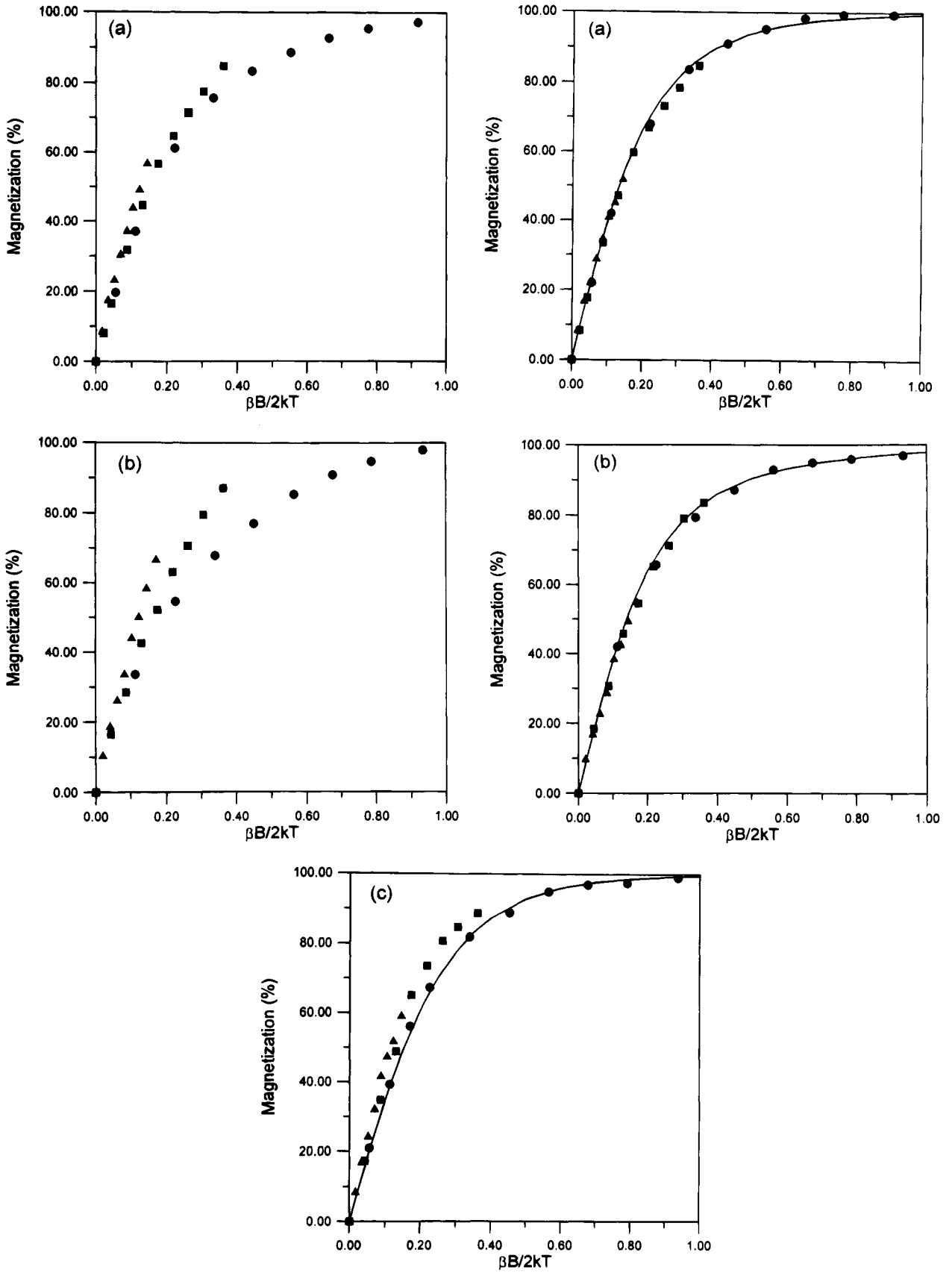

Figure 8. MCD magnetization data for Co(II)-substituted HLADH derivatives: (a) Co(c)Zn(n)-HLADH at 662 nm; (b) Co(c)Zn(n)-HLADH/NAD^+/pyrazole ternary complex at 674 nm. (c) Zn(c)Co(n)-HLADH at 733 nm. In each case, the magnetic field was varied from 0 to 4.5 T at 1.66 K (●), 4.22 K (■), and 9.5 K (▲). The left panels show the data as collected, and the right panels show the data after subtraction of a temperature-independent *B*-term contribution commensurate with the fits to the corresponding MCD temperature dependence data; see Figure 7. The solid lines are theoretical magnetization curves originating from an isolated doublet ground state, computed using eq 7 with $g_{\parallel} = 6.5$, $g_{\perp} = 1.9$, and $m_z/m_{xy} = -0.2$ for Co(c)Zn(n)-HLADH; $g_{\parallel} = 7.1$, $g_{\perp} = 0.3$, and $m_z/m_{xy} = -0.2$ for the Co(c)Zn(n)-HLADH/NAD^+/pyrazole ternary complex; and $g_{\parallel} = 2.2$, $g_{\perp} = 4.6$, and $m_z/m_{xy} = -0.2$ for Zn(c)Co(n)-HLADH.

of the magnitude of the zero-field splittings determined for Co(c)Zn(n)-HLADH and Co(c)Zn(n)-HLADH/NAD$^+$/pyrazole, only the ground state doublet should be significantly populated at temperatures up to 10 K. Hence, to a first approximation, the magnetization data can be analyzed in terms of *C*-term and temperature-independent *B*-term contributions from the lower doublet. In both cases, subtraction of a *B*-term contribution, scaled according to the magnitude of that required in fitting the temperature dependence data at the same wavelength (see Figure 7) eliminates the nesting and gives rise to type of magnetization data expected for a *C*-term originating from a magnetically isolated Kramers doublet (Figure 8, right panels). Theoretical expressions are then available to analyze such data for a randomly oriented axial chromophore in terms of the effective *g*-values and the transition polarization:[44]

$$\Delta\epsilon \propto m_{xy}^2\left\{\int_0^{\pi/2}\frac{\cos^2\theta\sin\theta}{\Gamma}g_{\parallel}\tanh\left(\frac{\Gamma\beta B}{2kT}\right)d\theta - \sqrt{2}\frac{m_z}{m_{xy}}\int_0^{\pi/2}\frac{\sin^3\theta}{\Gamma}g_{\perp}\tanh\left(\frac{\Gamma\beta B}{2kT}\right)d\theta\right\} \quad (5)$$

$$\Gamma = \sqrt{(g_{\parallel}^2\cos^2\theta + g_{\perp}^2\sin^2\theta)}$$

Orientation averaging is accomplished by numerical integration over θ, the angle between the molecular *z* axis and the applied field, and m_z and m_{xy} are the transition dipole moments for the molecular *z*- and *xy*-polarized transitions. Since the effective *g*-values for the lower doublet are known from the EPR measurements, fitting the data to eq 5 gives an estimate of the transition polarization ratio, m_z/m_{xy}. In both cases a good fit can be obtained using the EPR-determined *g*-values and $m_z/m_{xy} = -0.2$, suggesting that these transitions are predominantly *xy*-polarized, which is in good agreement with the single-crystal polarization studies of Co(c)Zn(n)-HLADH.[41]

The absence of *B*-term contributions and the closer spacing of the ground state doublets in the case of Zn(c)Co(n)-HLADH suggest that the nesting of the magnetization data is a consequence of population of the upper doublet. For a zero-field splitting of 7 cm^{-1}, the Boltzmann population of the upper doublet is 0.2%, 9%, and 35% at 1.66 K, 4.2 K, and 9.5 K. Since the *C*-term from the upper doublet is approximately twice the magnitude of that from the lower doublet at this wavelength (see Figure 7c), the observed increase in the initial slope of the magnetization data with increasing temperature is readily rationalized. Only the lowest doublet is significantly populated at 1.66 K, and the magnetization at this temperature is well fit by theoretical data constructed for the EPR-determined effective *g*-values, $g_{\parallel} = 2.2$ and $g_{\perp} = 4.6$, with $m_z/m_{xy} = -0.2$, suggesting that the transition is predominantly *xy*-polarized.

Discussion

The results presented herein represent the first attempt to analyze both the ground and excited state properties of high-spin Co(II) in biological samples using the combination of VTMCD and EPR spectroscopies. In particular, protocols have been developed for analyzing MCD magnetization data in terms of ground state g-values and transition polarization and for determining the ground state zero-field splitting from plots of MCD intensity against $1/T$ in the linear limit. More detailed understanding of the excited state properties and extraction of ligand field parameters will require near-IR VTMCD measurements to identify the components of the $^4A_2 \rightarrow {}^4T_1(F)$ d−d band. Such experiments with Co(II)-HLADH derivatives and other Co(II)-substituted Zn proteins are in progress in this laboratory, and the results will be reported elsewhere.

For the Co(II)-substituted HLADH derivatives investigated in this work, i.e. Co(c)Zn(n)-HLADH and Zn(c)Co(n)-HLADH and their ternary complexes with NAD$^+$ and pyrazole, the EPR and UV/visible absorption and VTMCD spectra are readily interpreted in terms of tetrahedral coordination at the Co site. The EPR spectra can be understood in the framework of an $S = {}^3/_2$ spin Hamiltonian with anisotropic intrinsic *g*-values in the range characteristic of tetrahedral Co(II) complexes, i.e. $g = 2.1-2.4$. The average energy of the components of the $^4A_2 \rightarrow {}^4T_1(P)$ d−d band lies in the range established for tetrahedral Co(II) complexes, i.e. 14 000−18 000 cm^{-1},[15] and the molar extinction coefficients for the most intense component are >300 M^{-1} cm^{-1}, which is also indicative of tetrahedral coordination.[15,19,38] Moreover, the change in the average energy of this d−d band with the change in the ligand donor set is in complete accord with the order of ligands in the spectrochemical series. The large splittings of the $^4A_2 \rightarrow {}^4T_1(P)$ d−d band that are observed for the samples with Co(II) at the catalytic site indicate a highly distorted coordination geometry. This is also indicated by the large ground state zero-field splittings which result from mixing of the low-lying $^4T_2$ excited state with the orbitally degenerate $^4A_2$ ground state via second-order spin−orbit coupling. The magnitude of the ground state zero-field splitting therefore correlates with the splitting of this excited state and will increase with spin−orbit coupling and the extent and nature of the low-symmetry distortion.[15,27]

One of the major objectives of this study was to reconcile the conflicting interpretations of optical absorption and X-ray crystallographic studies with the EPR spin relaxation measurements with respect to the Co(II) coordination number in binary and ternary complexes. All the currently available optical absorption and X-ray crystallographic data for binary and ternary complexes of native HLADH and Co(c)Zn(n)-HLADH indicate that Zn or Co at the catalytic site is in a distorted tetrahedral coordination environment.[7,10,17,19,20] Although an X-ray structure is not available for the Co(c)Zn(n)-HLADH/NAD$^+$/pyrazole ternary complex, there is a structure for the corresponding derivative of the native enzyme which shows the pyrazole nitrogen bound in place of the water oxygen atom.[45] In contrast, Makinen and co-workers have inferred pentacoordination at the catalytic Co(II) site in binary complexes with NAD$^+$ and NADH and several ternary complexes, including the Co(c)Zn(n)-HLADH/NAD$^+$/pyrazole ternary complex, on the basis of the magnitude of ground state zero-field splitting as determined by EPR from the temperature dependence of the spin−lattice relaxation.[26] One obvious means of reconciling the conflicting results was to invoke a change in Co coordination number on freezing samples for EPR. However, the low-temperature absorption and VTMCD studies reported here rule out this possibility. Moreover, the excellent agreement between the solution and single-crystal absorption studies of Co(c)Zn(n)-HLADH demonstrate that no structural changes are associated with crystallization.[41] Hence the low-temperature spectroscopic data need to be interpreted in light of the X-ray crystal structure of Co(c)Zn(n)-HLADH, which shows a highly distorted tetrahedral environment at the catalytic Co site.[16]

The present work raises two problems with the zero-field-splitting approach for assessing the coordination number of Co(II) in biological samples. The first concerns the reliability of zero-field splittings determined by the temperature dependence of EPR saturation behavior. The values determined for Co(c)Zn(n)-HLADH and Co(c)Zn(n)-HLADH/NAD$^+$/pyrazole from MCD studies, $|\Delta| = 33$ cm^{-1} and $\Delta = -56$ cm^{-1},

(45) Eklund, H.; Samama, J.-P.; Wallén, L. *Biochemistry* **1982**, *21*, 4858−4866.

respectively, are very different from those determined by the EPR method, $\Delta = +9$ and $+47$ cm^{-1}, respectively. In the latter case, the value must be considered as inherently unreliable since the EPR spectrum used for the determination does not correspond to that of the Co(c)Zn(n)-HLADH/NAD$^+$/pyrazole ternary complex. The discrepancy for Co(c)Zn(n)-HLADH is less easy to explain. The EPR method relies on the assumption that electron spin relaxation occurs exclusively via an Orbach relaxation mechanism over a small and ill-defined temperature range (e.g. 4−7 K in the case of Co(c)Zn(n)-HLADH). Moreover, the method has proven unreliable for negative axial zero-field splittings, $D < 0$, and it is unclear how the measurement is affected by a rhombic field, $E/D \approx 0.33$, as is the case in Co(c)Zn(n)-HLADH. The MCD measurement does not depend on the spin relaxation mechanism or nature of the ground state distortion and is solely a function of the Boltzmann population distribution over the doublets of the ground state manifold. However, it does require fitting to an expression involving five variable parameters. Such procedures are inherently unreliable without constraints or independent assessment of some of the parameters. This is provided by the MCD magnetization studies which provide an independent assessment of the *B*-term contribution at low temperatures and by studies at different wavelengths, since only the MCD *C*- and *B*-term parameters will be wavelength dependent. For these reasons, we consider the MCD−determined values of high-spin Co(II) zero-field splittings to be more reliable, although clearly more MCD studies of magnetically well-characterized Co(II) complexes are called for to check the validity of protocols developed herein.

This then leads to second problem, namely that the zero-field splittings obtained for Co(c)Zn(n)-HLADH and Co(c)Zn(n)-HLADH/NAD$^+$/pyrazole via MCD measurements are outside the range established for tetrahedral Co(II) centers on the basis of single-crystal polarized absorption, EPR, or magnetic susceptibility measurements of a handful of structurally defined Co(II) samples, i.e. Δ between -36 and $+13$ cm^{-1} for tetracoordinate sites, between $+20$ and $+50$ cm^{-1} for pentacoordinate sites of trigonal bipyramidal or square pyramidal geometry, and $\geq +50$ cm^{-1} for hexacoordinate sites.[27] The trend in the magnitude of the zero-field splitting is predicted on theoretical grounds and is logical, given the change from a orbitally nondegenerate ground state that is split by second-order spin−orbit coupling in the case of tetrahedral coordination to an orbitally degenerate ground state that is split by first-order spin−orbit coupling in the case of octahedral coordination. However, the range quoted for tetrahedral complexes is based largely on measurements of Co(II) doped into host lattices where the environments are more homogeneous and less distorted than the catalytic Co site in Co(c)Zn(n)-HLADH. The X-ray crystal structure of Co(c)Zn(n)-HLADH shows that the Co is coordinated by two cysteines, one histidine, and one water molecule in a highly distorted tetrahedral arrangement; e.g. the S−Co−S angle is 130° and the N−Co−O angle is 102°.[16] On the basis of the crystal structure for the NAD$^+$/pyrazole ternary complex of the native Zn-HLADH, which shows a S−Zn−S angle of 129° and a N−Zn−N angle is 91°,[45] it is likely the pyrazole binding in place of H_2O results in an even larger distortion from idealized tetrahedral geometry at the catalytic Co site. Theoretical calculations predict that such large distortions, coupled with the heterogeneous ligand environment, will give rise to anomalously large (positive or negative) zero-field splittings, well outside the range quoted above for tetrahedral coordination.[15] Hence it seems likely that these ranges for the magnitude of the ground state zero-field splitting are not appropriate for highly distorted tetracoordinate Co(II) sites.

That the MCD measurement gives reliable estimates of Co(II) zero-field splittings is further supported by the value obtained for Co(II) in the noncatalytic site of HLADH, i.e. 7 cm^{-1}. Although no crystal structure is available for Zn(c)Co(n)-HLADH, the noncatalytic Zn site in native HLADH is coordinated by four cysteines with the S−Zn−S angles deviating by only a few degrees from perfect tetrahedral geometry.[7] A similar coordination environment for Co(II) in the noncatalytic site is indicated by the splitting of the $^4T_1$(P) excited state which is readily interpreted in terms of first-order spin−orbit coupling with only minor contributions from low-symmetry distortions. Hence a small ground state zero-field splitting is expected and observed.

Overall we conclude that the magnitude of the Co(II) zero-field splitting does not always provide a reliable method for distinguishing between four tetracoordinate and pentacoordinate Co(II) atoms in low-symmetry biological environments. Notwithstanding, small values, $|\Delta| < 20$ cm^{-1}, can be used as criteria for tetracoordinate Co(II). For predominantly axial systems, the sign of Δ (best determined by EPR temperature dependence studies) can provide an additional criteria, since $D < 0$ is only possible for tetracoordinate Co(II). In general, it is clearly desirable to integrate optical absorption, VTMCD, and EPR results in reaching a definitive conclusion concerning coordination number for Co(II) in highly distorted environments, rather than relying on any one technique alone.

At this juncture it is worthwhile to briefly review and critique the other spectroscopic methods that have been used to distinguish between tetracoordinate and pentacoordinate Co(II) in biological systems. The form of the room-temperature MCD spectrum has been extensively used following the empirical relationships established in the pioneering work of Vallee and co-workers.[46] For tetrahedral complexes, the MCD under the $^4A_2 \rightarrow {}^4T_1$(P) transition is biphasic with the negative band to lower energy and close to the absorption maximum. In contrast for five-coordinate complexes, the split components of the transition to the P levels generally all exhibit negative MCD bands. This generalization appears to hold remarkably well. For example it applies to the high-temperature MCD for the Co-HLADH samples investigated in this work; see Figures 3−5. However, the VTMCD results reported here indicate that it should be used with caution, since the room-temperature MCD of highly distorted tetrahedral Co(II) centers is dominated by oppositely signed *B*-terms whereas the *C*-terms corresponding to the transitions to the low-symmetry components of the excited state are negative in sign. Likewise the empirical relationship between the maximum extinction coefficient of the visible d−d band and the coordination number, i.e. ϵ between 50 and 300 M^{-1} cm^{-1} for five-coordinate and $\epsilon > 300$ M^{-1} cm^{-1} for four-coordinate,[15,19,38] appears to be a generally reliable "rule-of-thumb". It has also been suggested that ^{59}Co hyperfine splitting is larger in octahedral and square pyramidal Co(II) complexes and that the observation of resolvable hyperfine splitting in the X-band EPR spectrum is therefore an indication of pentacoordinate or hexacoordinate Co(II).[47] Pilbrow[48] and Banci *et al.*[15] have demonstrated that the ratio of the ^{59}Co coupling constant and the effective *g*-value for each principal direction remains approximately constant. This explains why ^{59}Co hyperfine

(46) Kaden, T. A.; Holmquist, B.; Vallee, B. L. *Inorg. Chem.* **1974**, *13*, 2585−2590.
(47) Bencini, A.; Bertini, I.; Canti, G.; Gatteschi, D.; Luchinat, C. *J. Inorg. Biochem.* **1981**, *14*, 81−91.
(48) Pilbrow, J. R. *Transition Ion Electron Paramagnetic Resonance*; Oxford University Press: Oxford, U.K., 1990.

splitting, if observed, is generally only apparent on the low-field resonance. Hence the likelihood of seeing resolvable hyperfine structure depends critically on the ground state properties, but not necessarily on the coordination number. The EPR results presented here for Co(c)Zn(n)-HLADH (see Figure 2) provide a dramatic illustration that well-resolved ^{59}Co hyperfine splitting can be observed for Co(II) in a distorted tetrahedral environment.

A brief comment is appropriate in connection with the assignment of the visible absorption spectrum of Co(II)-substituted HLADH. Throughout, we have attributed the bands in the 500−800 nm region to components of the highest energy spin-allowed ligand field transition, $^4A_2 \rightarrow {}^4T_1(P)$. However, on the basis of single-crystal polarized absorption measurements and extended Hückel molecular orbital calculations, Makinen and co-workers have argued that these visible absorption bands are predominantly S-to-Co(II) CT as opposed to ligand field in origin.[41] Although we agree that mixing with low-energy CT transitions is likely to be responsible for the intensity enhancement of these bands, the conventional assignment has been retained in this work since the intensity of these bands in tetrahedral Co(II) complexes is not particularly sensitive to the nature of the ligands and the energies of the visible and near-IR bands are readily rationalized in terms of a ligand field analysis.[49,50]

As well as enhancing current understanding of the ground and excited state properties of Co(II) in low-symmetry biological environments, the results provide further insight into the properties of HLADH. The insensitivity of the EPR and low-temperature MCD characteristics of Co(II) in the noncatalytic site to inhibitor binding at the catalytic site and the change from the open to the closed conformation supports a purely structural role for the noncatalytic Zn in HLADH. In addition, the results show no indication of a change in coordination number at the catalytic Co(II) site on formation of the closed ternary complex with NAD^+ and pyrazole. While more MCD studies on a wider variety of Co(c)Zn(n)-HLADH derivatives are required, the results reported here, combined with the available optical data, support the view that the catalytic Co(II) site is tetracoordinate in all derivatives except those involving bidentate inhibitors such as 1,10-phenanthroline.[20] While this does not rule out the possibility of pentacoordinate intermediates, it supports the view that active-site metal remains tetracoordinate throughout the catalytic cycle.

Acknowledgment. This work was supported by grants from the National Science Foundation (DMB9419019 and DIR9012481 to M.K.J.), the National Institutes of Health (GM33806 and GM51962 to M.K.J.), the Deutsche Forschungsgemeinschaft, Schwerpunktprogramm Bioanorganische Chemie, and the Fonds der Chemischen Industrie.

IC9407656

(49) Carlin, R. L. In *Transition Metal Chemistry*; Carlin, R. L., Ed.; Marcel Dekker: New York, 1965; Vol. 1, pp 1−32.

(50) Bailar, J. C.; Emelius, H. J.; Nyholm, S. R.; Trotman-Dickerson, A. F. *Comprehensive Inorganic Chemistry*; Pergamon Press: New York, 1973; pp 1087−1093.